EXTENDED GRIPPING CONDITIONS OF ROCK CLIMBER-LIKE ROBOT FOR ASYMMETRIC GRIPPING CONFIGURATION IN MICROGRAVITY

*Kyohei Maruya[1], Yudai Yuguchi[2], Wudom Tesshin[3], Kenji Nagaoka[4], and Kazuya Yoshida[5]

[1] *Tohoku University, Aoba 6-6-01, Aramaki, Aoba-ku, Sendai, Japan, E-mail: maruya@astro.mech.tohoku.ac.jp*
[2] *Tohoku University, Aoba 6-6-01, Aramaki, Aoba-ku, Sendai, Japan, E-mail: yuguchi@astro.mech.tohoku.ac.jp*
[3] *Tohoku University, Aoba 6-6-01, Aramaki, Aoba-ku, Sendai, Japan, E-mail: u-dom@astro.mech.tohoku.ac.jp*
[4] *Tohoku University, Aoba 6-6-01, Aramaki, Aoba-ku, Sendai, Japan, E-mail: nagaoka@astro.mech.tohoku.ac.jp*
[5] *Tohoku University, Aoba 6-6-01, Aramaki, Aoba-ku, Sendai, Japan, E-mail: yoshida@astro.mech.tohoku.ac.jp*

ABSTRACT

An advanced robotic locomotion mechanism is required for exploring a minor body which has irregular surfaces in a microgravity environment. In this paper, we propose a rock climber-like robot that can perform with accurate mobility on an unknown minor body. One of the technological requirements for the robot is a gripping mechanism that can grip tightly on an uneven surface. To meet this requirement, the gripping conditions must be theoretically derived. This paper presents the conditional equations for the grippable range on an irregular surface based on friction theory, and the validation of the developed equations experimentally using an air-floating test bed system.

1 INTRODUCTION

Exploration of minor bodies such as asteroids or comets has received a lot of attention in recent years. Minor bodies are expected to hold clues that can reveal the state of the primary solar system and its evolutionary process. They are also regarded as possible targets for manned explorations in future, and hence, it is useful to investigate them. To enhance the achievements of the exploration of minor bodies, using small robots that can move on their surfaces is an effective exploration method. Furthermore, from a viewpoint of scientific interest, the robots are required to reach destinations where scientific attention would be high. However, there are technical difficulties in the accomplishment of robotic locomotion on minor bodies because of two characteristic conditions: the gravity on the minor body is extremely small, and the minor body has an unknown irregular terrain. In such conditions, it is difficult for a robot to maintain contact with the surface. In particular, traditional wheeled or tracked robots can easily hop by the reaction force from the surface.

For an asteroid exploration robot, hopping mobility has been studied as an effective method of exploration. MINERVA is a representative asteroid exploration robot, which was carried in the Japanese spacecraft Hayabusa [1]. Following MINERVA, MINERVA-II1 [2] and MINERVA-II2 [3] were developed and equipped in the Hayabusa 2 spacecraft that is cruising on its target path. These robots can move by the reaction forces or torques generated by built-in actuators. However, the hopping robots have difficulties in reaching the desired destination precisely, because they do not have soft-landing mechanisms, and thus the destination depends very much on the surface conditions. In contrast, Yoshida et al. [4] proposed a rock climber-like robot that can move on a minor body by gripping its surface, as shown in Figure 1. This locomotion method enables the robot to reach the destination by continuous stable locomotion. For the realization of this robot system, two technical challenges should be addressed: One is robust gait control for stable locomotion on a rough terrain in a microgravity environment, and the other is reliable gripping control for holding on an irregular surface. This paper presents information on how the latter is addressed.

To date, some researchers have studied robotic gripping mechanisms in a microgravity environment. The NASA/JPL's robotics group proposed the robot LEMUR IIB and conducted gripping experiments using a prototyped robot [5]. Its gripping mechanism is composed of 256 sharp hooks and flexible elements to grip the surface of a rock. This is a super-redundant mechanism, and hence the friction characteristics of the contact points can be ignored during its gripping phase. However, the gripper was not getting released easily from the surface, and the hooks broke frequently [6]. Research on gripping mechanisms for base-fixed manipulators has been conducted for ground applications. The unidirectional nature of the constraints by using fingers was addressed in the analysis of form closure [7] and force closure [8]. The contact dynamics between the fingers and the objects was also analyzed [9, 10]. Furthermore, stability analysis of gripping against a disturbance applied to the gripped object was performed [11]. Yuguchi et al. [12] have applied the

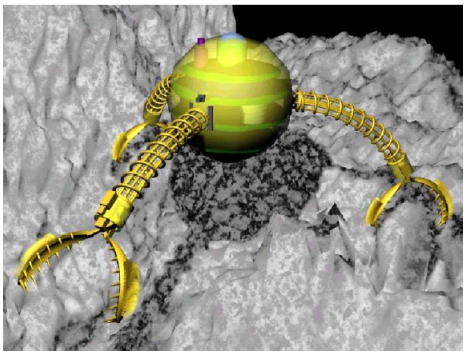

Figure 1 : Conceptual illustration of rock climber-like robot

gripping analysis to the rock climber-like robot moving on a minor body. They derived the static ground gripping characteristics in a microgravity environment based on the manipulation theory established with the theory of polyhedral convex cones [13]. In addition to the theoretical analysis, they evaluated the characteristics experimentally, where the relative positions of the ground surface and the gripping points were assumed to have symmetrical configuration. However, for practical applications, the gripping characteristics must be extended to asymmetric gripping conditions.

This paper presents an extended theory of the ground gripping conditions in asymmetrical configuration. The extended theory is a generalized framework for evaluating the gripping capability of the rock climber-like robot. The theory is validated based on experiments with planar motion in a microgravity environment using an air-floating test bed system.

2 GRIPPING CAPABILITY ANALYSIS

While gripping the ground surface, the inclination angle of the surface and the coefficient of friction at the contact point have a large influence on the gripping capability. We define gripping capability in terms of an equation that gives the conditions under which the gripping mechanism can generate a constant gripping force without slippage. This section presents the theory of static gripping conditions, including asymmetric configuration of the relative positions in a microgravity environment.

2.1 Formulation of Gripping Conditions

Given that the robot is in a static condition, the reaction force $\boldsymbol{f}$ and gravitational force $\boldsymbol{W}$ exerted on the robot, are as shown in Figure 2. Here, $\boldsymbol{f_{iB}}$ ($i = 1, 2, \cdots, n$) is the reaction force on the i-th finger and the subscript $\mathbf{B}$ indicates that the variable is defined in the coordinate system fixed on the robot base $\Sigma_B\{x_\mathrm{B}, y_\mathrm{B}\}$. Furthermore, $\boldsymbol{x_{iB}}$ is the position vector from the center of gravity of the robot to the tip of the i-th finger. The equilibrium equations of the reaction force and the moment around the center of gravity can be expressed as follows.

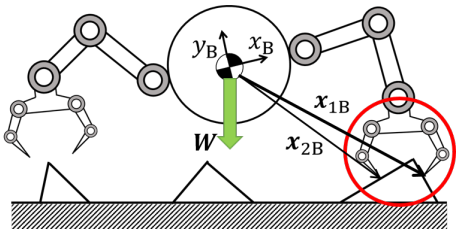

(a) Overall view of the robot

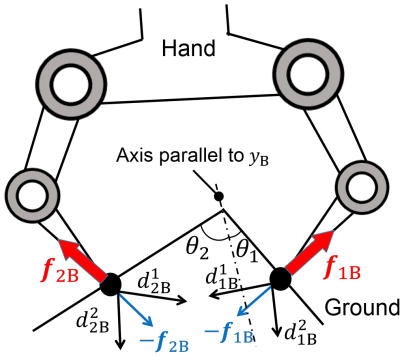

(b) Gripping state of the hand

Figure 2 : Asymmetric gripping state of ground grip locomotive robot in Σ_B

$$\sum_{i=1}^{n} \boldsymbol{f_{iB}} = -\boldsymbol{W} \tag{1}$$

$$\sum_{i=1}^{n} \boldsymbol{x_{iB}} \times \boldsymbol{f_{iB}} = \mathbf{0} \tag{2}$$

To satisfy the equilibrium conditions, the gripping force $-\boldsymbol{f_{iB}}$ on the ground surface must be generated inside of the frictional cone without slip on the ground. Thus, we approximate the frictional cone as a polyhedral cone. We define the edge vectors of the polyhedral cone for the i-th finger as $\boldsymbol{d^1_{iB}}$, $\boldsymbol{d^2_{iB}}$, ... , $\boldsymbol{d^m_{iB}}$, where $\boldsymbol{m}$ is the number of the edge line of the polyhedral cone. Consequently, the condition that $-\boldsymbol{f_{iB}}$ works inside the polyhedral cone is given as follows.

$$\exists R^j_{i\mathrm{B}} \geq 0 \quad \text{s.t.} \quad \sum_{j=1}^{m} R^j_{i\mathrm{B}} \boldsymbol{d^j_{iB}} = -\boldsymbol{f_{iB}} \tag{3}$$

Accordingly, Eq. (3) provides the no-slip condition for the i-th finger. In addition, substituting Eq. (3) into Eqs. (1) and (2), the gripping conditions are re-written as follows.

$$\exists R^j_{i\mathrm{B}} \geq 0 \quad \text{s.t.} \quad \sum_{i=1}^{n}\sum_{j=1}^{m} R^j_{i\mathrm{B}} \boldsymbol{d^j_{iB}} = \boldsymbol{W} \tag{4}$$

$$\sum_{i=1}^{n}\sum_{j=1}^{m} R^j_{i\mathrm{B}} \boldsymbol{d^j_{iB}} \times \boldsymbol{x_{iB}} = \mathbf{0} \tag{5}$$

2.2 Analysis of Possible Gripping Range the Ground

In this study, we assume the robot to be a dual-arm robot model in two dimensions for simplification, i.e., $n = m = 2$. Moreover, μ is the coefficient of static friction between the ground and the tip of the robot, and the gravity force $\boldsymbol{W}$ is assumed to be zero because of microgravity. θ_1 and θ_2 (where $-\pi \leq \theta_1 \leq \pi$ and $-\pi \leq \theta_2 \leq \pi$) are the inclined angles of the gripping surface with respect to the y_B axis, as shown in Figure 2. A counter-clockwise direction indicates a positive angle, and thus in Figure 2, θ_1 is positive and θ_2 is negative. For simplification, we define $2\phi \equiv \theta_1 - \theta_2$, and rotate the base coordinate system by $(\theta_1 + \theta_2)/2$, as shown in Figure 3. In the rotated coordinate system $\Sigma_\phi\{x_\phi, y_\phi\}$, the y_ϕ axis is in the same direction as the bisector of the inclination angle of the ground. From this definition, Eqs. (4) and (5) can be re-written with respect to the y_ϕ axis as follows.

$$\exists R^j_{i\phi} \geq 0 \quad \text{s.t.} \quad \sum_{i=1}^{2}\sum_{j=1}^{2} R^j_{i\phi}\boldsymbol{d^j_{i\phi}} = \boldsymbol{0} \tag{6}$$

$$\sum_{i=1}^{2}\sum_{j=1}^{2} R^j_{i\phi}\boldsymbol{d^j_{i\phi}} \times \boldsymbol{x_{i\phi}} = \boldsymbol{0} \tag{7}$$

On the basis of the geometric relationship shown in Figure 3, the edge vectors of the polyhedral cone $\boldsymbol{d^j_{i\phi}}$ can be given as follows.

$$\begin{aligned} \boldsymbol{d^1_{1\phi}} &= \begin{bmatrix} -\cos(\phi-\alpha) \\ -\sin(\phi-\alpha) \end{bmatrix}, \ \boldsymbol{d^1_{2\phi}} = \begin{bmatrix} -\cos(\phi+\alpha) \\ -\sin(\phi+\alpha) \end{bmatrix} \\ \boldsymbol{d^2_{1\phi}} &= \begin{bmatrix} \cos(\phi-\alpha) \\ -\sin(\phi-\alpha) \end{bmatrix}, \ \boldsymbol{d^2_{2\phi}} = \begin{bmatrix} \cos(\phi+\alpha) \\ -\sin(\phi+\alpha) \end{bmatrix} \end{aligned} \tag{8}$$

where $\alpha = \tan^{-1}\mu$ represents the half-angle of the friction cone. Substituting Eq. (8) into Eqs. (6) and (7), the following simultaneous inequalities are obtained.

$$\begin{cases} -x_{21\phi}\sin(\phi+\alpha) + y_{21\phi}\cos(\phi+\alpha) \leq 0 \\ x_{21\phi}\sin(\phi-\alpha) - y_{21\phi}\cos(\phi-\alpha) \leq 0 \\ x_{21\phi}\sin(\phi+\alpha) + y_{21\phi}\cos(\phi+\alpha) \geq 0 \\ x_{21\phi}\sin(\phi-\alpha) + y_{21\phi}\cos(\phi-\alpha) \leq 0 \end{cases} \tag{9}$$

where $\boldsymbol{x_{1\phi}} \equiv \begin{pmatrix} x_{1\phi} & y_{1\phi} \end{pmatrix}^{\mathrm{T}}$, $\boldsymbol{x_{2\phi}} \equiv \begin{pmatrix} x_{2\phi} & y_{2\phi} \end{pmatrix}^{\mathrm{T}}$, $x_{21\phi} \equiv x_{1\phi} - x_{2\phi}$, and $y_{21\phi} \equiv y_{1\phi} - y_{2\phi}$. By solving Eq. (9), the gripping capability can be finally determined as follows.

$$\alpha - \phi \geq 0 \tag{10}$$

$$-(\alpha-\phi) \leq \sin^{-1}\left(\frac{y_{21\phi}}{\sqrt{x^2_{21\phi}+y^2_{21\phi}}}\right) \leq \alpha - \phi \tag{11}$$

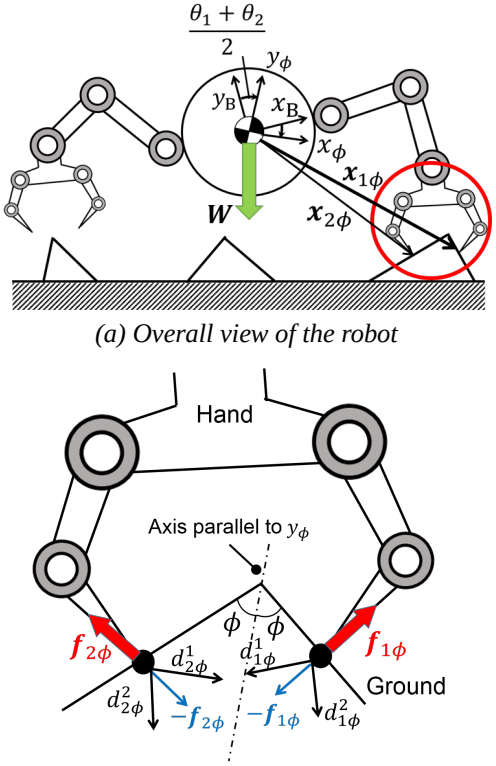

(a) Overall view of the robot

(b) Gripping state of the hand

Figure 3 : Asymmetric gripping state of ground grip locomotive robot in Σ_ϕ

From Eqs. (10) and (11), it can be said that there exist a maximum inclination angle of the surface and a range of gripping points for positive gripping. Here, $\sin^{-1}\left(y_{21\phi}/\sqrt{x^2_{21\phi}+y^2_{21\phi}}\right)$ represents the slope between the two fingertips in Σ_ϕ. Therefore, once $\boldsymbol{x_{1\phi}}$ is decided, the possible range of $\boldsymbol{x_{2\phi}}$ for gripping the ground surface is limited, as shown in Figure 4.

Additionally, the expression Eq. (11) can be obtained in Σ_B by rotating Σ_ϕ again through $-(\theta_1+\theta_2)/2$ as follows.

- $\theta_1 \geq \theta_2$:

$$-\theta_2 - \alpha \leq \sin^{-1}\left(\frac{y_{21\mathrm{B}}}{\sqrt{x^2_{21\mathrm{B}}+y^2_{21\mathrm{B}}}}\right) \leq \alpha - \theta_1 \tag{12}$$

- $\theta_1 \leq \theta_2$:

$$-\theta_2 - \alpha + \pi \leq \sin^{-1}\left(\frac{y_{21\mathrm{B}}}{\sqrt{x^2_{21\mathrm{B}}+y^2_{21\mathrm{B}}}}\right) \leq \alpha - \theta_1 - \pi \tag{13}$$

where $\boldsymbol{x_{1\mathrm{B}}} \equiv \begin{pmatrix} x_{1\mathrm{B}} & y_{1\mathrm{B}} \end{pmatrix}^{\mathrm{T}}$, $\boldsymbol{x_{2\mathrm{B}}} \equiv \begin{pmatrix} x_{2\mathrm{B}} & y_{2\mathrm{B}} \end{pmatrix}^{\mathrm{T}}$, $x_{21\mathrm{B}} \equiv x_{1\mathrm{B}} - x_{2\mathrm{B}}$, and $y_{21\mathrm{B}} \equiv y_{1\mathrm{B}} - y_{2\mathrm{B}}$.

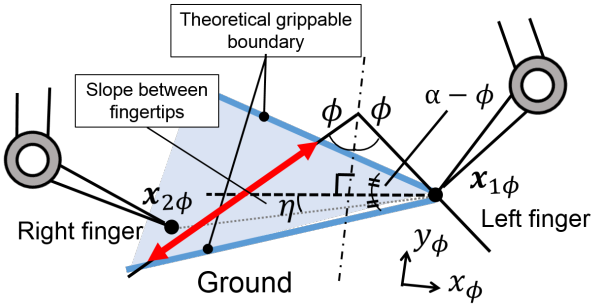

Figure 4 : Schematic view of the grippable range

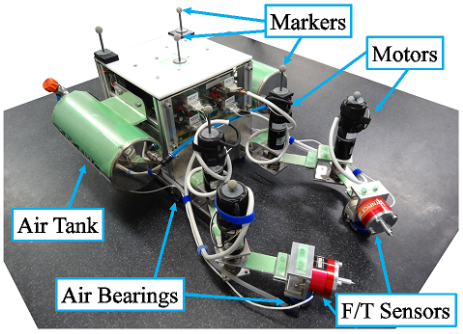

Figure 5 : Air-floating test bed system

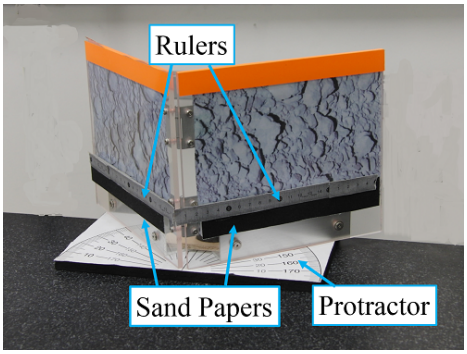

Figure 6 : Simulated ground

3 GRIPPING EXPERIMENT

This section presents the gripping experiments conducted on the simulated ground using an air-floating test bed system. The range of grippable points is determined by the point at which the fingers slip on the surface. The theoretical results are verified through comparison with the experimental results.

3.1 Air-Floating Test Bed System

To evaluate the gripping performance in a microgravity environment, we developed the air-floating test bed system, which is shown in Figure 5. This system performs planar motion in a microgravity environment using air bearings and air tanks. Frictionless motion can be simulated between the system and the surface plate. Moreover, this system has a dual-arm which has two motor-driven joints and a six-axis force/torque sensor in each arm. The driving motors (RH-8D-3006-E100AL) are produced by Harmonic Drive Systems Inc., and the force/torque sensors (WDF-6M200-3) are produced by WACOH-TECH Inc. On each force/torque sensor, a specific finger mechanism is attached. The system can measure the data of the reaction force while gripping the surface. The motion of the system is measured by a motion capture system (OptiTrack FLEX:V100R2) produced by NaturalPoint Inc., and the measured data is used as the basic information.

3.2 Simulated Ground

Figure 6 shows a view of the simulated ground. The simulated ground is composed of two flat plates and these are connected by two passive hinges. The inclination angle between the two plates can be changed arbitrarily. Furthermore, sandpapers are attached on the surface of the plates to simulate various frictional surfaces. In the experiments, the simulated ground was fixed on a flat plane using clamps.

3.3 Experimental Condition

Figure 7 shows an overview of the experimental setup. In the experiments, the range of the relative position of the fingertips for stable gripping was investigated by examining the boundary at which the fingertips begin to slip. According to the experimental results by Yuguchi et al. [12], a cone-shaped finger is more effective for gripping. Therefore, we also used cone-shaped fingers in the experiments, as shown in Figure 8. The material of the fingers is SUS304. The fingers were contacted in a direction perpendicular to the ground. Moreover, the fingertips were controlled to move with a constant velocity, and the motion was stopped when the reaction forces were greater than 1.5 N for safe operation. For the simulated ground, #100 sandpaper was used. The coefficient of static friction between the sandpaper and the tip of cone-shaped fingers was obtained from the measured data as follows [12].

$$\mu = 3.08$$

To verify the derived theory, we conducted experiments in five different conditions of the inclination angles of the simulated ground: $\phi = 55°, 60°, 65°, 70°$ and $75°$. From Eq. (10) and with $\mu = 3.08$, the maximum inclination angle for gripping was calculated as $72°$. Here, we define η as the slope between the fingertips. In the experiments, the left finger was fixed at a position 7 cm from the top of the simulated ground. Then, the contact position of the right finger was changed so that η changes with increments of $1°$. The experiments in each condition were conducted five times. The acceleration due to gravity was set to 0.016 G.

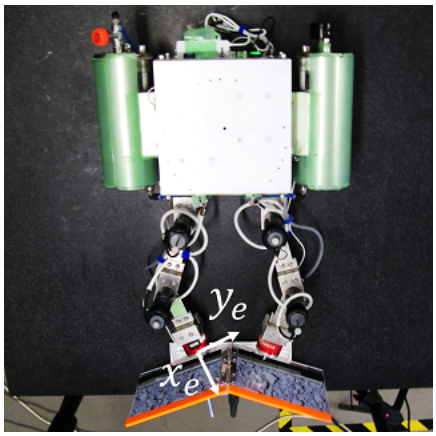

Figure 7 : Experimental setup of the robot and the simulated ground

Figure 8 : Cone-shaped finger

3.4 Experimental Results

Figure 9 shows the theoretical and experimental results on gripping capability for several slopes between the fingertips. The blue lines and the red cross marks indicate the theoretical values and experimental results, respectively. In the case of $\phi = 55°$ in Figure 9(a), the theoretical grippable range can be calculated from Eq. (11) as follows.

$$-17° \leq \eta \leq 17°$$

It may be noted that $\eta = 0$ means that the arrangement of the system and the simulated ground is symmetrical. Furthermore, Figures 10 and 11 show the time history of the reaction forces. These graphs show that the force increased and became constant at a value greater than 1.5N in the case of successful gripping; on the other hand, the force was not generated or was reduced to zero in the case of failure to grip. Therefore, the gripping capability was determined by the reaction force.

From Figures 9(a)~(d), it can be seen that the grippable range is narrower in the experiments than in the theoretical results. In addition, we conducted the test for the case of $\phi = 75°$ and $\eta = 0$, a case in which it is impossible to grip the surface. The result of this case was that the robot was not able to grip the surface during any of the five attempts. Considering the practical applications, we define the grippable boundary as the angle η at which the robot was able to grip during all the five attempts. With this definition, the theoretical and experimental values of

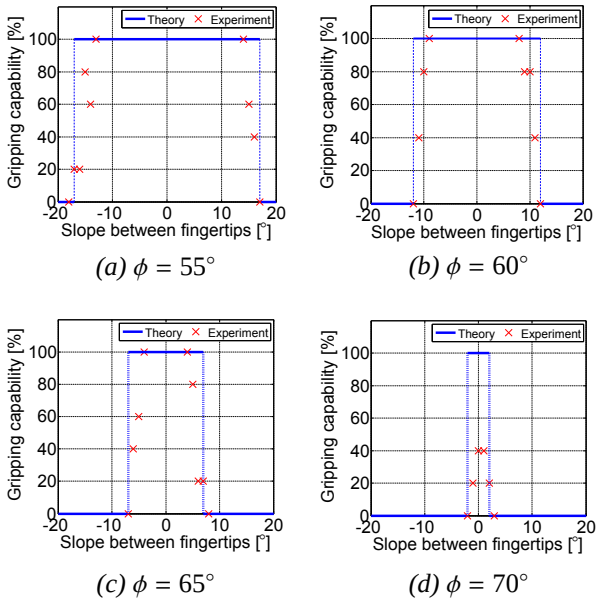

Figure 9 : Comparison of theoretical and experimental gripping capabilities

the grippable range are shown in Table 1. A comparison of the theoretical and experimental grippable ranges for various inclination angles of the simulated ground is shown in Figure 12. From Table 1 and Figure 12, it can be seen that in case when the inclination angle is between 55° and 65°, the value of the absolute error in each grippable boundary angle was within 4°. In the case of $\phi = 70$, there was no grippable point in the experiment, though the theoretical grippable boundary angle is ±4°. Moreover, the deviations in the experimental and the theoretical values increased with increase in the inclination angle. From these results, it can be seen that regardless of the magnitude of the inclination angle, the test bed system has an error of $6° \sim 7°$ in the grippable range η. These errors occurred based on the accuracy of the friction coefficients measured and the positioning accuracy of the manipulator joints including the mechanical parts and motors. However, these errors are small, and thus the validity of the derived theory was confirmed. The rock climber-like robot can achieve gripping locomotion on a minor body in practical applications, if sufficient margin is considered for the gripping boundary.

4 CONCLUSION

This study evaluated the extended static gripping conditions of a rock climber-like robot in asymmetric gripping configuration of the relative positions of the ground and the gripping points in a microgravity environment. The gripping capability was analyzed based on the experimental results and theoretical analysis. As a result, it was found that there is a relationship between the inclination angle of the ground and the range of gripping points for

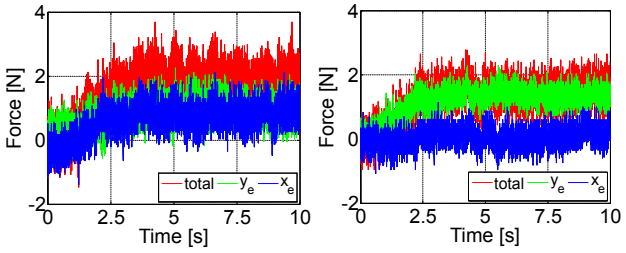

(a) Left fingertip *(b) Right fingertip*

Figure 10 : Reaction forces in the case of successful gripping ($\phi = 55°, \eta = -13°$)

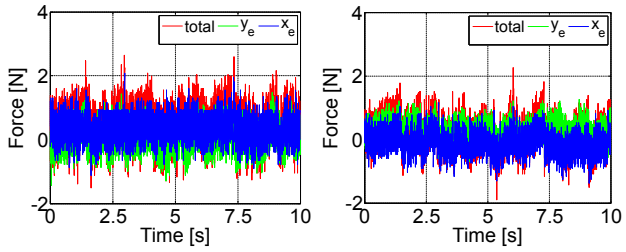

(a) Left fingertip *(b) Right fingertip*

Figure 11 : Reaction forces in the case of failure to grip ($\phi = 75°, \eta = 0°$)

positive gripping. Then, in the gripping experiments using an air-floating test bed system, the validity of the conditional equations for the grippable range was verified. In future research, it is necessary to evaluate the gripping capability on a real rough terrain.

Table 1 : Theoretical and experimental values of the grippable range

ϕ	Theory	Experiment	Absolute error
55°	$-17° \le \eta \le 17°$	$-13° \le \eta \le 14°$	$3° \sim 4°$
60°	$-12° \le \eta \le 12°$	$-9° \le \eta \le 8°$	$3° \sim 4°$
65°	$-7° \le \eta \le 7°$	$-4° \le \eta \le 4°$	3°
70°	$-2° \le \eta \le 2°$	Failure	-
75°	Failure	Failure	-

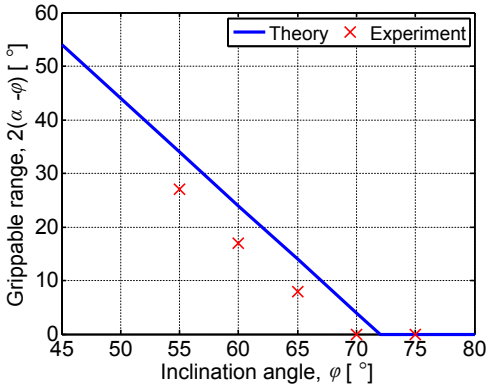

Figure 12 : Comparison of the theoretical and experimental grippable ranges for various inclination angles

References

[1] T. Yoshimitsu, T. Kubota, et al. (2003), "Micro-Hopping Robot for Asteroid Exploration", *Acta Astronautica*, vol. 52, pp. 441–446.

[2] T. Yoshimitsu, T. Kubota, , et al. (2014), "Development of Hopping Rovers for a New Challenging Asteroid", *Proceedings of the 12th International Symposium on Artificial Intelligence, Robotics and Automation in Space*, #5C-01.

[3] K. Nagaoka, K. Yoshida, et al. (2015), "Development of MINERVA-II2, a Micro-Robot for Asteroid Surface Exploration with Innovative Mobility", *The 11th Low-Cost Planetary Missions Conference*, Berlin, Germany.

[4] K. Yoshida, T. Maruki, et al. (2002), "A Novel Strategy for Asteroid Exploration with a Surface Robot", *Proceedings of the 34th COSPAR Scientific Assembly*, pp. 281–286.

[5] A. Parness, M. Frost, et al. (2012), "Gravity-independent Mobility and Drilling on Natural Rock Using Microspines", *Proceedings of 2012 IEEE International Conference on Robotics and Automation*, pp. 3437–3442.

[6] A. Parness, M. Frost, et al. (2013), "Gravity-independent Rock-climbing Robot and a Sample Acquisition Tool with Microspine Grippers", *Journal of Field Robotics*, vol. 30, no. 6, pp. 897–915.

[7] K. Lakshminarayana (1978), "Mechanics of Form Closure", *ASME Technical report*, no. 78-DET-32.

[8] V. Nguyen (1988), "Constructing Force- Closure Grasps", *The International Journal of Robotics Research*, vol. 7, no. 3, pp. 3–16.

[9] J. Kerr and B. Roth (1986), "Analysis of Multifingered Hands", *The International Journal of Robotics Research*, vol. 4, no. 4, pp. 3–17.

[10] P. Akella and M. Cutkosky (1989), "Manipulating with Soft Fingers: Modeling Contacts and Dynamics", *Proceedings of the 1989 IEEE International Conference on Robotics and Automation*, vol. 2, pp. 764–769.

[11] A. Nakanishi and Y. Hayakawa (2011), "Stability Analysis of Multi-Fingered Grasp under Destabilizing Gravity Effect", *Proceedings of the 18th World Congress The International Federation of Automatic Control*, vol. 12, pp. 14667–14674.

[12] Y. Yuguchi, W. F. R. Ribeiro, et al. (2015), "Experimental Evaluation of Gripping Characteristics Based on Frictional Theory for Ground Grip Locomotive Robot on an Asteroid", *Proceedings of the 2015 IEEE International Conference on Robotics and Automation*, pp. 2822–2827.

[13] S. Hirai and H. Asada (1993), "Kinematics and Statics of Manipulation Using the Theory of Polyhedral Convex Cones", *The International Journal of Robotics Research*, vol. 12, no. 5, pp. 434–447.